



Cubature rules with positive weights on union of disks

Alvise Sommariva^a · Marco Vianello^a

Abstract

In this work we present a new algorithm that computes cubature formulas with positive weights, interior nodes and fixed algebraic degree of precision, over domains Ω that are arbitrary union of disks. This novel approach first determines the boundary $\partial\Omega$ and then defines a decomposition of Ω by means of nonoverlapping circular segments and polygons, where algebraic positive interior rules can be locally constructed. The resulting global Positive Interior (PI) formula is finally compressed by Caratheodory-Tchakaloff subsampling implemented via NonNegative Least-Squares.

1 Introduction

Numerical modelling by finite collections of arbitrary disks/balls is relevant in several different applications. Problems involving disk/ball intersection, union and difference arise for example in computational optics, wireless network analysis, computational chemistry (Van der Waals molecular modelling); see, e.g., [1, 3, 12, 14, 15, 26] with the references therein. A basic problem is the computation of areas and volumes of such sets, followed by the more difficult task of computing integrals on them by suitable cubature formulas, in particular algebraic formulas (i.e., with a given degree of polynomial exactness) having positive weights and interior nodes (PI-formulas).

In the recent paper [20] we have constructed low-cardinality algebraic PI-formulas on arbitrary disk intersections, the main tools being subdivision of the intersection into nonoverlapping asymmetric circular sectors, PI algebraic cubature on such sectors via subperiodic trigonometric Gaussian quadrature [5], and cubature compression via Caratheodory-Tchakaloff subsampling implemented by NonNegative Least Squares [16]. This work was apparently the first systematic approach to the algebraic cubature problem on disk intersections, and contained also an approach for disk union, via a basic implementation of the inclusion-exclusion principle, which however suffers of exponential complexity and is prone to produce a huge number of nodes and negative weights.

The disk intersection cubature problem, though nontrivial, is somehow simplified by the fact that the intersection is a convex curvilinear polygon, whose sides are circular arcs. In this paper, we cope the more difficult disk union cubature problem, whose core is boundary tracking of the resulting intrinsically nonconvex (and possibly multiply connected) curvilinear polygon.

The main lines of the construction are the following. Let $\Omega = \cup_s B(P_s, r_s)$ an arbitrary finite union of closed planar disks centered at P_s with radius r_s . First, we split Ω into its connected components (that are disk sub-unions), namely $\Omega = \cup_k \Omega_k$. Notice that some of the Ω_k can be multiply connected if such is Ω . Then, by a boundary tracking algorithm that solves the delicate problem of detecting the arc components, we are able to split each Ω_k into the nonoverlapping union of circular segments $S_{k,j}$ (disk portions corresponding to a cut by a straight line) and of a single simple polygon \mathcal{P}_k (possibly multiply connected if such is Ω_k), obtaining eventually

$$\Omega = \cup_s B(P_s, r_s) = \cup_k ((\cup_j S_{k,j}) \cup \mathcal{P}_k), \quad (1)$$

see Figure 1 and also Figure 2 to have an idea of the variety of possible configurations. From this splitting we obtain the algebraic cubature formulas exact for every polynomial $p \in \mathbb{P}_n^2$

$$\iint_{\Omega} p(\mathbf{x}) d\mathbf{x} = \sum_{k,j,h} \lambda_{k,j,h} p(\mathbf{x}_{k,j,h}) + \sum_{k,l} \lambda_{k,l} p(\mathbf{x}_{k,l}) = \sum_{i=1}^M \lambda_i p(\mathbf{x}_i) = \sum_{\ell=1}^m w_{\ell} p(\xi_{\ell}), \quad \{\xi_{\ell}\} \subset \{\mathbf{x}_i\} = \{\mathbf{x}_{k,j,h}\} \cup \{\mathbf{x}_{k,l}\} \subset \Omega, \quad \lambda_i, w_{\ell} > 0, \quad (2)$$

where the first equality comes from the collection of PI-formulas on circular segments [7] and linear polygons (cf. e.g. [2]), the second one is simply a renumbering of the overall set of M corresponding nodes, and the third one corresponds to cubature compression via Caratheodory-Tchakaloff subsampling implemented by NonNegative Least Squares, where a subset of nodes is extracted and re-weighted preserving the polynomial degree of exactness [16]. We stress that $m \leq \dim(\mathbb{P}_n^2) = (n+1)(n+2)/2 < M$ and $m \ll M$ for the union of a large number of disks (the ratio M/m being roughly proportional to such a number).

In Section 2 we focus on the boundary tracking problem for arbitrary disk unions, that leads in Section 3 to the construction of high-cardinality PI-formulas by splitting into nonoverlapping circular segments and linear polygons. Such formulas can be conveniently compressed via NonNegative Least Squares applied to the underdetermined moment system, as shown in Section 4. Finally, in Section 5 we present some numerical experiments on disk unions with quite complex shape.

^aUniversity of Padova, Italy

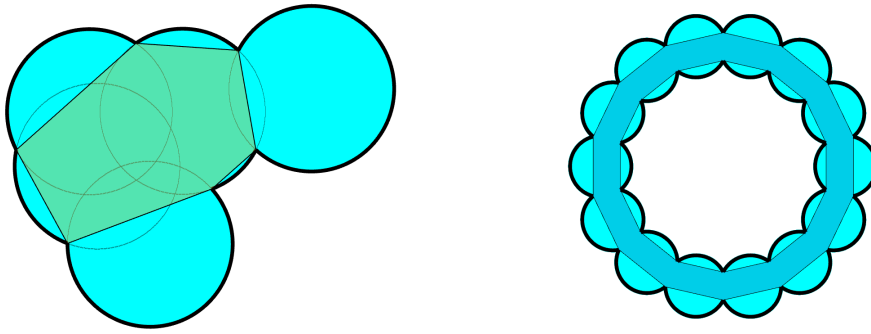


Figure 1: Simply (left) and multiply connected (right) disk union with their nonoverlapping splittings into circular segments and polygon.

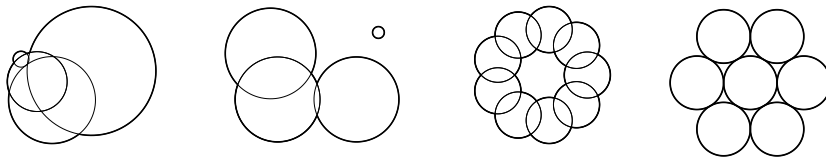


Figure 2: Examples of domains Ω that are unions of disks. From left to right a simply connected domain, a disconnected domain, a multiply connected domain and finally one with disks that are tangent.

2 Boundary tracking

In this section we intend to determine the boundary $\partial\Omega$, where $\Omega = \cup_{k=1}^K B(P_k, r_k)$. This result will be one of the key points for providing an algebraic cubature rule on Ω with positive weights and internal nodes. To understand the difficulty of this analysis, in Figure 2 we illustrate four very different domains Ω , i.e., from the left to the right, a simply connected, a disconnected, a multiply connected domain and finally one with seven disks that are tangent.

To this purpose, the simplest case is given two disks $B_1 = B(P_1, r_1)$, $B_2 = B(P_2, r_2)$ respectively with centers P_1, P_2 and radii r_1, r_2 . First define the interval of angular coordinates $I_{B_1, B_2} \subseteq [0, 2\pi)$ such that

$$\partial B_1 \cap \partial(B_1 \cup B_2) = \{(x, y) : x = P_1(1) + r_1 \cos(\theta), y = P_1(2) + r_1 \sin(\theta), \theta \in I_{B_1, B_2}\}.$$

In other words, I_{B_1, B_2} is the set of angular coordinates in the range $[0, 2\pi)$ w.r.t P_1 , center of the disk B_1 , of the portion of the boundary of $\partial(B_1 \cup B_2)$ that is also in ∂B_1 .

Observe that

- in general, I_{B_1, B_2} is a pluri-interval (union of disconnected intervals): for example, in Figure 3 $I_{B_1, B_2} = [0, \pi/4] \cup [5\pi/4, 2\pi)$;
- if $B_1 \cap B_2 = \emptyset$ then $I_{B_1, B_2} = [0, 2\pi)$;
- if ∂B_1 and ∂B_2 are tangent in a point T then if $B_1 \subset B_2$

$$\partial B_1 \cap \partial(B_1 \cup B_2) = \partial B_1 \cap \partial B_2 = T$$

and thus I_{B_1, B_2} consists of the angular value of the polar coordinates of T with respect to P_1 , otherwise

$$\partial B_1 \cap \partial(B_1 \cup B_2) = \partial B_1$$

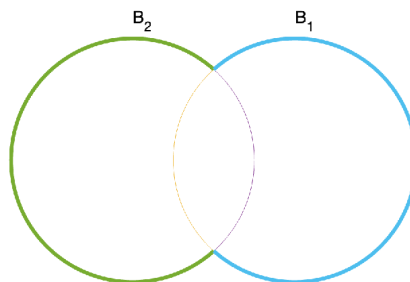


Figure 3: In this example, the set I_{B_1, B_2} corresponds to the angles determining the arc in cyan, i.e. $I_{B_1, B_2} = [0, \pi/4] \cup [5\pi/4, 2\pi)$. The set I_{B_2, B_1} corresponds to the angles determining the arc in green, i.e. $I_{B_2, B_1} = [\pi/4, 7\pi/4]$.

and $I_{B_1, B_2} = [0, 2\pi)$.

- in general, in view of its definition, I_{B_1, B_2} may not be equal to I_{B_2, B_1} , indeed in Figure 3 $I_{B_2, B_1} = [\pi/4, 7\pi/4]$.

In the more general case of $\Omega = \cup_{k=1}^K B_k$ where $B_k := B(P_k, r_k)$, it is not difficult to see that the portion of ∂B_k that is in $\partial\Omega$ corresponds to

$$\partial B_k \cap \partial\Omega = \{(x, y) : x = P_k(1) + r_k \cos(\theta), y = P_k(2) + r_k \sin(\theta), \theta \in I_k := \cap_{l \neq k} I_{B_k, B_l}\}$$

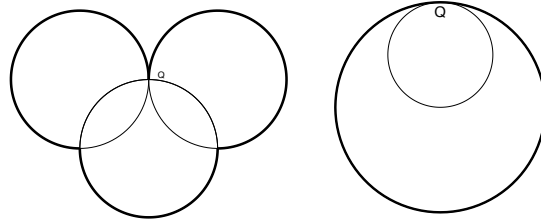


Figure 4: Left: Example of a disk, the *lower one*, with an isolated point Q belonging to the boundary of the union of disks. Right: Example of a disk, the *inner one*, with an isolated point Q belonging to the boundary of the union of disks.

Also notice that I_k is in general a pluri-interval, i.e. the union of some disconnected subintervals of $[0, 2\pi)$, some of which may actually be isolated points and in this case they can be dropped since they actually do not contribute to the determination of $\partial\Omega$. In view of this last observation, we will define I_k^* as I_k without isolated points. It is easy to see that the set I_k^* may be:

- equal to the empty set and in this case the disk B_k is completely in the interior of or has some point belonging to the boundary that does not add any contribution to the definition of $\partial\Omega$;
- equal to $[0, 2\pi)$, i.e the interior of the disk B_k does not intersect the interior of any other disk;
- union of disconnected intervals $I_{k,1}^*, \dots, I_{k,\mu_k}^*$ where we can suppose after a suitable reordering that $\max I_{k,j}^* < \min I_{k,j+1}^*$ for $j = 1, \dots, \mu_k - 1$, and in particular none of them are isolated points.

Applying the same procedure to all the disks B_k , $k = 1, \dots, K$, we get all the sets $\partial B_k \cap \partial\Omega$, $k = 1, \dots, K$ in terms of $I_k = \cap_{j=1}^{\mu_k} I_{B_k, B_j}$ and next I_k^* after purging I_k of possible isolated points. As previously stated, we can suppose that the pluri-interval I_k^* can be described as $I_k^* = \cup_{j=1}^{\mu_k} I_{k,j}^*$ where $\max I_{k,j}^* < \min I_{k,j+1}^*$ for $j = 1, \dots, \mu_k - 1$.

At this point we can also require that all the disks B_k provide some not empty sets I_k^* , otherwise they do not give any contribution to the determination of $\partial\Omega = \partial(\cup_{k=1}^K B_k)$ and can be dropped without any consequence.

Now we intend to determine the boundary of each connected component of Ω as a sequence of arcs, each one having intersection with the next one only on its final extrema. To help the reading, see Figure 4.

Let

$$\gamma_{k,j} := \{(x, y) : x = P_k(1) + r_k \cos(\theta), y = P_k(2) + r_k \sin(\theta), \theta \in I_{k,j}^*\},$$

for $k = 1, \dots, K, j = 1, \dots, \mu_k$ be the arcs defining the boundary. Furthermore let $I_{k,j}^* = [a_{k,j}, b_{k,j}]$ and set

$$\gamma_{k,j}^{(1)} = (P_k(1) + r_k \cos(a_{k,j}), P_k(2) + r_k \sin(a_{k,j}))$$

$$\gamma_{k,j}^{(2)} = (P_k(1) + r_k \cos(b_{k,j}), P_k(2) + r_k \sin(b_{k,j})),$$

i.e. the two extremal points of the arc $\gamma_{k,j}$, for $k = 1, \dots, K, j = 1, \dots, \mu_k$.

Letting $\Gamma_{1,1} = \gamma_{1,1}$, we have two possibilities:

- $\gamma_{1,1}^{(1)} = \gamma_{1,1}^{(2)}$ in which case we have determined a closed arc $\Gamma_1 := \gamma_{1,1}^{(1)}$ of $\partial\Omega$, i.e. an arc where the first and final extrema coincide, that is the whole boundary of an isolated disk;
- $\gamma_{1,1}^{(1)} \neq \gamma_{1,1}^{(2)}$ in which case, by construction, there is exactly one arc, say $\Gamma_{1,2} := \gamma_{k,j}$ such that $\gamma_{k,j}^{(1)} = \gamma_{1,1}^{(2)}$.

This procedure can be iterated until for a certain L_1 the last extrema of the arc Γ_{1,L_1} is equal to the first extrema of $\Gamma_{1,1}$.

At this point, if no arc is available, i.e. all the arcs $\gamma_{k,j}$, $k = 1, \dots, K, j = 1, \dots, \mu_k$ took part in the process, then we have determined the boundary of $\partial\Omega$ and it corresponds to $\Gamma_1 = \cup_{i=1}^{L_1} \Gamma_{1,i}$, otherwise we pick randomly one of the missing $\gamma_{k,j}$ and repeat the procedure to compute Γ_2 and if necessary, $\Gamma_3, \dots, \Gamma_\nu$, until all the arcs $\gamma_{k,j}$, $k = 1, \dots, K, j = 1, \dots, \mu_k$ took part of the process.

Notice that, since the single circle arcs are counterclockwise tracked, as a result whatever is the order of the disks in the union, the outer boundaries are counterclockwise tracked, as well as in the multiply connected case the inner boundaries are clockwise tracked; see Figure 1 to have an idea.

When the procedure ends, we have determined the boundary of the domain, as $\partial\Omega = \cup_{i=1}^\nu \Gamma_i$, i.e. of ν possibly disconnected and closed curves, each being piecewise arcs.

Some of the main worries of this algorithm concern how it treats some pathological cases:

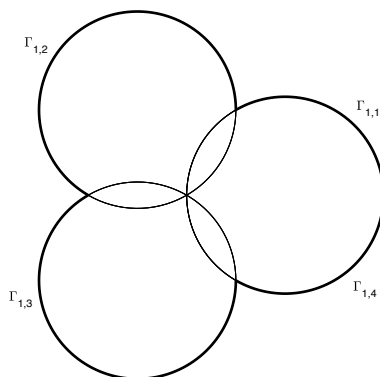


Figure 5: Union of disks and arcs determining its boundary. The first arc $\Gamma_{1,1}$ has the red dot as first extremal point $\gamma_{1,1}^{(1)}$.

- two connected closed arcs Γ_i, Γ_j , with $i \neq j$, are somewhere tangent: in this case, the boundary is still defined correctly, as consequence of the fact that if two disks are tangent then $I_{B_1, B_2}^* = I_{B_2, B_1}^* = \emptyset$;
- Ω is not a connected region: the algorithm detects correctly its boundaries since in two disconnected regions all the arcs in the first one are not connected to arcs in the second one, so providing two different Γ_k .

3 Construction of algebraic PI-formulas on union of disks

Once that the boundary $\partial\Omega$ is described via its closed curves $\Gamma_1, \dots, \Gamma_\nu$, that are its outer and inner boundaries, we are ready to determine the cubature formula. For the sake of simplicity, we initially suppose that each of its possibly disconnected components Ω_k are simply connected, so that $\Gamma_k = \partial\Omega_k$ are outer boundaries.

We seek an algebraic PI-formula with Algebraic Degree of Exactness $ADE = n$. In view of the additivity of the integral, this is immediately obtained by collection of PI-formulas with $ADE = n$ on each Ω_k , and in turn these can be obtained by nonoverlapping splitting of Ω_k .

Indeed, we start observing that Ω_k is the union of say L_k circular segments and a polygon \mathcal{P}_k . More precisely, since $\Gamma_k = \cup_{j=1}^{L_k} \Gamma_{k,j}$ for some arcs $\Gamma_{k,1}, \dots, \Gamma_{k,L_k}$, letting $\Gamma_{k,j}^{(1)}, \Gamma_{k,j}^{(2)}$ the extrema of each $\Gamma_{k,j}$ (ordered counterclockwise), we have that Ω_k is the union of

1. the circular segments $S_{k,j}$, $j = 1, \dots, L_k$ whose boundary is defined by $\Gamma_{k,j}$ and the linear segment connecting $\Gamma_{k,j}^{(2)}$ with $\Gamma_{k,j}^{(1)}$,
2. the polygon \mathcal{P}_k whose sides are the segments obtained by connecting $\Gamma_{k,j}^{(1)}$ with $\Gamma_{k,j}^{(2)}$ for $j = 1, \dots, L_k$.

Notice that taken any two of these circular segments cannot overlap, otherwise there would be an arc portion of one segment, that is a portion of the boundary of Ω , contained in the interior of another, that is in the interior of Ω . This also implies that \mathcal{P}_k is a simple polygon, otherwise we would have two overlapping circular segments.

We are now ready to determine a cubature formula on Ω_k . Again, by additivity of the integral, it is sufficient to have an algebraic PI-formula with $ADE = n$ on the circular segments $S_{k,j}$ and on the simple polygon \mathcal{P}_k .

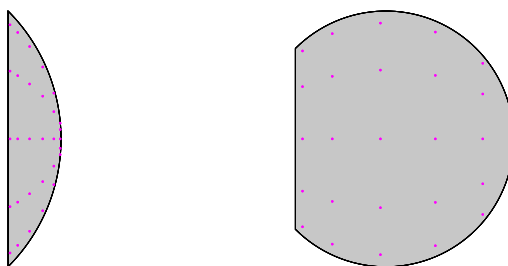


Figure 6: Product Gaussian quadrature nodes of algebraic exactness degree $n = 6$ on two circular segments with angular extension $\pi/2$ (left) and $3\pi/2$ (right).

Concerning circular segments, by no loss of generality (up to a rotation and a translation) we can consider a circular segment, say S , of a disk centered at the origin with radius r , corresponding to a vertical cut with angular extension say 2σ , $0 < \sigma < \pi$; see Figure 6. Then following [7], by the injective transformation $\mathbf{x}(u, \theta) = (r \cos(\theta), ru \sin(\theta))$, $u \in [-1, 1]$, $\theta \in [0, \sigma]$, and the same with $\theta \in [-\sigma, 0]$, both with Jacobian $r^2 \sin^2(\theta)$, we get the cubature formula of product Gaussian type

$$\iint_S p(\mathbf{x}) d\mathbf{x} = \frac{1}{2} \int_{-1}^1 \int_{-\sigma}^{\sigma} p(\mathbf{x}(u, \theta)) r^2 \sin^2(\theta) d\theta du = \sum_{s=1}^{\lceil \frac{n+1}{2} \rceil} \sum_{t=1}^{\lceil \frac{n+2}{2} \rceil} \lambda_{s,t} f(\mathbf{x}_{s,t}) = \sum_{h=1}^{\lceil \frac{n+1}{2} \rceil \lceil \frac{n+2}{2} \rceil} \lambda_h f(\mathbf{x}_h), \quad \forall p \in \mathbb{P}_n^2(S)$$

$$\lambda_{s,t} = r^2 \sin^2(\varphi_t) \omega_s z_t, \quad \mathbf{x}_{s,t} = (r \cos(\varphi_t), r u_s \sin(\varphi_t)), \quad (3)$$

where $\{(u_s, \omega_s)\}$ are the nodes and weights of the algebraic Gauss-Legendre formula for degree n in $[-1, 1]$, and $\{(\varphi_t, z_t)\}$ are the angular nodes and weights of the subperiodic trigonometric Gaussian formula for degree $n + 2$ in $[-\sigma, \sigma]$ developed in [6] (the last sum in h simply corresponds to a renumbering of the nodes). Indeed, the key points are that $p(\mathbf{x}(u, \theta)) \sin^2(\theta) \in \mathbb{P}_n([-1, 1]) \otimes \mathbb{T}_{n+2}[-\sigma, \sigma]$ that is the tensor product space of univariate algebraic polynomials of degree not exceeding n and univariate trigonometric polynomials of degree not exceeding $n + 2$ (where subperiodicity means that the trigonometric polynomials are restricted to a subinterval $[-\sigma, \sigma]$ of the period), and that the nodes are substantially repeated twice by symmetry. The corresponding Matlab code `gqcircsegm.m` can be found at [21].

Concerning the simple polygon \mathcal{P}_k , whose number of sides is L_k , i.e. the number of circular segments pertaining to Ω_k , we have adopted the algebraic cubature rule with positive weights and internal points on general polygons, even not simply connected or disconnected, implemented in [2]. In such cases, the corresponding algorithm determines a minimal triangulation of the polygon (via the Matlab `polyshape` and `triangulation` routines), with a number of triangles equal to $L_k - 2$, and then, by the best known rules over each triangle with $ADE = n$, a PI cubature formula on the whole polygon.

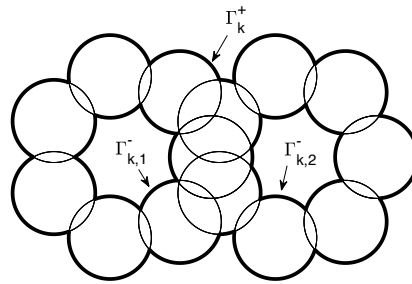


Figure 7: A multiply connected union and the definition of its boundary.

The case in which a component Ω_k is not simply connected is a little more complicated. Suppose that its outer boundary is Γ_k^+ while $\Gamma_{k,1}^-, \dots, \Gamma_{k,s_k}^-$ are the closed curves determining the inner boundaries, one for each possible *hole* (see Figure 7).

The component Ω_k is the union of

1. the circular segments defined by the arcs in Γ_k^+ ,
2. the circular segments defined by the arcs in each $\Gamma_{k,1}^-, \dots, \Gamma_{k,s_k}^-$,
3. the not simply connected polygon \mathcal{P}_k having as sides the segments connecting each of the previous arcs.

Observe that again $\partial \mathcal{P}_k$ does not cross itself, that is \mathcal{P}_k is a simple polygon with holes.

One of the possible difficulties, in the case of a not simply connected domain, consists in detecting the boundary of a connected but not simply connected component of Ω . Consider two closed curves Γ_1, Γ_2 . Let P_1, P_2 be respectively the polygons obtained by connecting the subsequent vertices of the arcs determining, respectively, Γ_1 and Γ_2 . Then, if P_1 contains in its interior a vertex of P_2 , necessarily Γ_2 is the boundary of a *hole* inside the region spanned by Γ_1 .

Once we have determined $\Gamma_k^+, \Gamma_{k,1}^-, \dots, \Gamma_{k,s_k}^-$, we can obtain a PI cubature formula on this subdomain, by a PI algebraic rule on the not simply connected polygon \mathcal{P}_k (having as outer vertices the extremal points of its ordered sequence of arcs, and as inner vertices the extremal points of the ordered sequence of arcs of each $\Gamma_{k,j}^-$, $j = 1, \dots, s_k$), and PI formulas constructed as described above on the remaining circular segments, whose union is the closure of $\Omega_k \setminus \mathcal{P}_k$.

The collection of all these PI cubature formulas provides eventually a PI cubature formula exact on \mathbb{P}_n^2

$$\iint_{\Omega} p(\mathbf{x}) d\mathbf{x} = \sum_{k,j,h} \lambda_{k,j,h} p(\mathbf{x}_{k,j,h}) + \sum_{k,l} \lambda_{k,l} p(\mathbf{x}_{k,l}) = \sum_{i=1}^M \lambda_i p(\mathbf{x}_i), \quad \forall p \in \mathbb{P}_n^2, \quad (4)$$

where the first sum corresponds to the collection of circular segments $\{S_{k,j}\}$ and the second to the collection of the (possibly multiply connected) polygons $\{\mathcal{P}_k\}$, whereas the final sum is simply a renumbering of the whole set of nodes. Notice that, denoting by $L = \sum_k L_k$ the overall number of circular segments (that is typically proportional to the number of disks, or more precisely to the number of disks which contribute to the boundary of the union), and recalling the classical lower bound [23] for a cubature formula with $ADE = n$ that is $\nu_n = \dim(\mathbb{P}_{[n/2]}^2) \approx (1 + n/2)(2 + n/2)/2 = (n + 2)(n + 4)/8$, we get that the cardinality of the polygon cubature formula is at least $(L - 2C)\nu_n \approx (L - 2C)(n + 2)(n + 4)/8$, where C denotes the overall number of connected components of the union. Then the overall cardinality M is at least of the order of $L(n + 1)(n + 2)/4 + (L - 2C)(n + 2)(n + 4)/8 > LN/2 + (L - 2C)N/4 = (3L/4 - C/2)N$. This possibly large cardinality M can be reduced to at most $N = \dim(\mathbb{P}_n^2)$ by Caratheodory-Tchakaloff subsampling, as described in the next subsection, obtaining a compression ratio of at least $3L/4 - C/2$.

3.1 Caratheodory-Tchakaloff subsampling

The possibility of reducing the cardinality of a PI cubature formula inserts in the more general problem of measure compression, that is finding a discrete representative with low-cardinality finite support of a given multivariate measure, keeping invariant a certain number of polynomial moments. Such a problem has a long history, dating back at least to V. Tchakaloff with his celebrated theorem in 1957 [24].

Technically, in the case of a starting discrete measure (like a cubature formula) with high-cardinality support $X = \{\mathbf{x}_1, \dots, \mathbf{x}_M\} \subset \mathbb{R}^d$ and positive point-masses array $\lambda = (\lambda_1, \dots, \lambda_m)$, the problem can be formulated as that of finding a subset of the support, say $\{\xi_1, \dots, \xi_m\} \subset X$ such that

$$\sum_{i=1}^M \lambda_i p(\mathbf{x}_i) = \sum_{\ell=1}^m w_\ell p(\xi_\ell), \quad \forall p \in \mathbb{P}_n^d,$$

or equivalently in matrix terms finding a sparse nonnegative solution $u \in \mathbb{R}^M$ of the underdetermined moment system

$$u \geq 0 : V^t u = b = V^t \lambda, \quad V = [p_j(\mathbf{x}_i)], \quad 1 \leq i \leq M, \quad 1 \leq j \leq N, \quad (5)$$

where V is a Vandermonde-like matrix in any total-degree polynomial basis $\text{span}(p_1, \dots, p_N) = \mathbb{P}_n^d$, and $b = (b_j) = (\sum_{i=1}^M \lambda_i p_j(\mathbf{x}_i))$ is the corresponding moment array. We recall that existence of a nonnegative solution u^* with a number of nonzeros $m \leq N$ is ensured by the well-known Caratheodory theorem [4] on conical linear combination of a set of $N < M$ vectors in \mathbb{R}^M , applied to the columns of V^t . The nonzero components of u^* then are the new weights $\{w_\ell\}$ associated to a reduced support $\{\xi_\ell\} \subset X$.

Over the past decade, there has been a renewed interest in the numerical as well as in the probabilistic literature on the solution of (5) by optimization algorithms, namely by Linear or Quadratic Programming; cf. e.g. [11, 16, 25] with the references therein. Here we adopt the NNLS (NonNegative Least-Squares) approach developed in [22, 16] that consists in solving

$$\text{compute } u^* : \|V^t u^* - b\|_2 = \min_{u \geq 0} \|V^t u - b\|_2, \quad (6)$$

by Matlab implementations of the well-known Lawson-Hanson active-set algorithm [13], which automatically determines a sparse solution to (6). Its application gives a residual $\epsilon = \|V^t u^* - b\|_2$ that is typically very small, say $< 10^{-14}$ for $n \leq 30$. We point out that there are several versions of NNLS codes available in Matlab. One is the built-in function `lsqnonneg`, based on the Lawson-Hanson algorithm while an open-source version is present in the package NNLSlab [18]. A new and promising acceleration of the Lawson-Hanson algorithm is implemented in the routine LHDM first discussed in [10], based on the concept of column selection by deviation maximization instead of standard column pivoting for QR factorizations (cf. also [8, 9] for a full theoretical and numerical analysis of the deviation maximization approach).

We can then conclude by stressing that by Caratheodory-Tchakaloff compression of the PI cubature formula for arbitrary disk union developed above, we are able to provide a final PI formula whose support is a subset of the original one, with cardinality not exceeding the dimension of the exactness polynomial space. The corresponding Matlab codes are freely available at [19].

Remark 1. It is worth obtaining an estimate of the convergence rate by the PI cubature formulas just derived, related to the integrand smoothness. Denoting by p_n^* the best uniform approximation polynomial in \mathbb{P}_n^2 to a continuous integrand f on Ω , we get easily the estimate

$$\begin{aligned} \left| \iint_{\Omega} f(\mathbf{x}) d\mathbf{x} - \sum_{\ell=1}^m w_\ell f(\xi_\ell) \right| &\leq \left| \iint_{\Omega} (f(\mathbf{x}) - p_n^*(\mathbf{x})) d\mathbf{x} \right| + \left| \iint_{\Omega} p_n^*(\mathbf{x}) d\mathbf{x} - \sum_{\ell=1}^m w_\ell p_n^*(\xi_\ell) \right| + \left| \sum_{\ell=1}^m w_\ell (p_n^*(\xi_\ell) - f(\xi_\ell)) \right| \\ &\leq \left(\text{area}(\Omega) + \sum_{\ell=1}^m w_\ell \right) \|f - p_n^*\|_{\infty, \Omega} = 2 \text{area}(\Omega) \|f - p_n^*\|_{\infty, \Omega} \end{aligned}$$

where we have used the fact that the formula is exact in \mathbb{P}_n^2 so that the second summand on the first row vanishes, and that the weights are positive. On the other hand

$$\|f - p_n^*\|_{\infty, \Omega} \leq c_k n^{-k} \left(n^{-1} \sum_{\alpha_1 + \alpha_2 = 0}^k \|\partial_x^{\alpha_1} \partial_y^{\alpha_2} f\|_{\infty, \Omega} + \sum_{\alpha_1 + \alpha_2 = k} \text{osc}_{\Omega}(\partial_x^{\alpha_1} \partial_y^{\alpha_2} f; 1/n) \right), \quad \forall f \in C^k(\Omega),$$

where osc_{Ω} is the oscillation on Ω of a continuous function, i.e. $\text{osc}_{\Omega}(g; h) = \sup\{|g(\mathbf{u}) - g(\mathbf{v})|, \mathbf{u}, \mathbf{v} \in \Omega, |\mathbf{u} - \mathbf{v}| \leq h\}$, and c_k is a positive constant. The convergence rate shown in the last bound is a consequence of a classical Jackson-like estimate for multivariate euclidean balls by Ragozin [17, Thm. 3.4, p. 164], via the immediate property that the maximum uniform error on a finite union is the maximum of the uniform errors on the single components.

4 Numerical experiments

The purpose of this section is to numerically compare the cubature rules obtained with the present algorithm with that implemented in [20] by the inclusion-exclusion principle, also reporting for the latter the presence of negative weights. Our numerical tests have been performed on a Apple M1 CPU with 16 GB of RAM, using Matlab R2022a. The open source codes are available at [19].

We consider three different domains, having a complicated geometry:

- the simply connected domain Ω_1 is the union of 15 random disks, with all the centers contained in the square $[0, 1] \times [0, 1]$ and random radii in $[0, 1]$ (see Figure 8-left);
- the domain Ω_2 is $\Omega_2^{(r_1)} \cup \Omega_2^{(r_2)}$, where $\Omega_2^{(r_j)}$, $j = 1, 2$, is the union of 19 disks with centers $P_k^{(r_j)} = (r_j \cos(\theta_k), r_j \sin(\theta_k))$, where $\theta_k = 2k\pi/19$, $k = 0, \dots, 18$ and radius equal to $r_j/4$, with $r_1 = 2$ and $r_2 = 4$; notice that the set is the disconnected union of two multiply connected unions (see Figure 8-center);
- the domain Ω_3 is the union of the sets $\Omega_3^{(1)}, \Omega_3^{(2)}$ defined as follows; letting $t_k = 5k/44$, $k = 0, \dots, 44$, the set $\Omega_3^{(1)}$ is the union of the disks with centers $P_k^{(1)} = (2.5 \cos(2t_k), 2t_k)$ and radius $r_k^{(1)} = 0.3$, while $\Omega_3^{(2)}$ is the union of the disks with centers $P_k^{(2)} = (2.5 \sin(2t_k), 2t_k)$ and radius $r_k^{(2)} = 0.3$; the set is connected but not simply connected (see Fig. 8-right).

In the Tables, varying the domains, we display the quality of the cubature rules, named F(ull), C(ompressed) and O(ld), on a sequence of exactness degrees. We may observe that:

- we get always $card_C = N = dim(\mathbb{P}_n^2) < card_F \ll card_O$ and remarkable compression ratios $card_F/card_C$ varying in the examples from about 4 to more than 100 (indeed we expect, as discussed above after formula (4), a ratio size of at least $3/4$ the number of circular segments involved);
- the number $negw_O$ of negative weights of the *old* formula implemented in [20] is a consistent fraction of the overall weights, and the stability parameter $\sigma_O = \sum |w_O| / \sum w_O$ (not reported for brevity), independently of the degree is $\sigma_O \approx 213.0$ on Ω_1 , $\sigma_O \approx 1.785$ on Ω_2 and $\sigma_O \approx 1.675$ on Ω_3 , while for both the new rules is always equal to 1 since all the weights are positive;
- we compare the moments with respect to the product Chebyshev basis of the smaller cartesian boxes containing the domains Ω_k , via the new rule and the compressed one (using LHDM for solving the NNLS problem), by means of the Root Mean-Square Deviation $RMSD_{FC} = \|b_F - b_C\|_2 / \sqrt{N}$ and $RMSD_{FO} = \|b_F - b_O\|_2 / \sqrt{N}$, both being extremely small with the first not far from machine precision and the second at most of the order of 10^{-12} ;
- CPU_F , CPU_C , CPU_O are the detected cputimes and show that: (i) the new rule for mild degrees is faster than that proposed in [20]; (ii) boundary tracking time (not reported for brevity) requires on average respectively 6e-3s, 3e-2s, 2e-1s; (iii) as expected, the compression stage becomes relevant when one increases the ADE.

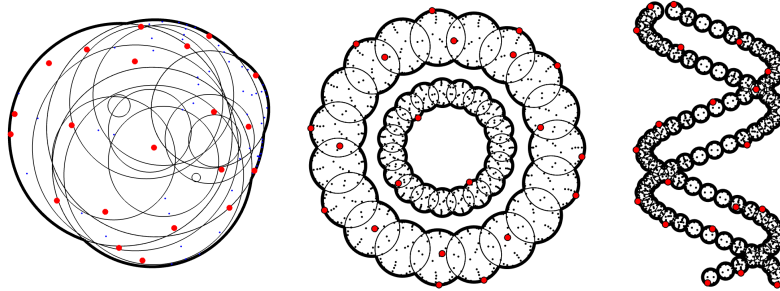


Figure 8: From left to the right, the domains $\Omega_1, \Omega_2, \Omega_3$ in which we perform our tests. In each of them we represent in black and red respectively the new cubature pointset and the compressed one, for $ADE = 5$.

Table 1: Comparison of cubature rules with $ADE n = 5, 10, 15, 20, 25$, on the disk union Ω_1 (F=Full, C=Compressed, O=Old).

ADE	$card_F$	$card_C$	$card_O$	$RMSD_{FC}$	$RMSD_{FO}$	$negw_O$	CPU_F	CPU_C	CPU_O
5	81	21	447584	$4e-16$	$2e-12$	223672	$4e-03$	$5e-03$	$1e+01$
10	252	66	1166652	$8e-16$	$2e-12$	583056	$4e-03$	$9e-03$	$2e+01$
15	498	136	2465379	$9e-16$	$1e-12$	1232082	$4e-03$	$4e-02$	$2e+01$
20	839	231	3921247	$1e-15$	$1e-12$	1959716	$4e-03$	$2e-01$	$3e+01$
25	1261	351	6103524	$1e-15$	$1e-12$	3050292	$6e-03$	$8e-01$	$4e+01$

5 Conclusion

We have implemented an algorithm that computes an algebraic Positive-Interior cubature formula on an arbitrary union of planar disks. The outcome of the algorithm gives several interesting information on such sets, that could be useful in applications where modelling by finite disk collections is adopted. In fact the algorithm:

- detects the connected components of the union;

Table 2: As in Table 1 for the disk union Ω_2 .

ADE	$card_F$	$card_C$	$card_O$	$RMSD_{F,C}$	$RMSD_{F,O}$	$negw_O$	CPU_F	CPU_C	CPU_O
5	1444	21	1632	$4e-14$	$8e-14$	1056	$6e-02$	$5e-02$	$9e-01$
10	4560	66	4896	$1e-14$	$4e-14$	3168	$6e-02$	$9e-02$	$9e-01$
15	8968	136	9792	$2e-14$	$2e-14$	6336	$6e-02$	$2e-01$	$9e-01$
20	15124	231	16456	$4e-14$	$1e-13$	10648	$6e-02$	$6e-01$	$9e-01$
25	22724	351	24752	$6e-14$	$1e-13$	16016	$8e-02$	$8e-01$	$9e-01$

Table 3: As in Table 1 for the disk union Ω_3 .

ADE	$card_F$	$card_C$	$card_O$	$RMSD_{F,C}$	$RMSD_{F,O}$	$negw_O$	CPU_F	CPU_C	CPU_O
5	2878	21	6824	$6e-15$	$9e-13$	3112	$2e-01$	$2e-01$	$3e+01$
10	9060	66	19224	$6e-15$	$1e-12$	9216	$2e-01$	$3e-01$	$3e+01$
15	17836	136	39384	$6e-15$	$9e-13$	18522	$2e-01$	$4e-01$	$3e+01$
20	30073	231	64614	$7e-15$	$9e-13$	30976	$2e-01$	$1e+00$	$3e+01$
25	45188	351	98644	$1e-14$	$9e-13$	46732	$3e-01$	$3e+00$	$3e+01$

- detects the outer and possible inner boundaries of each connected component (i.e. detects also the possible holes providing their boundary);
- constructs nodes and weights of a PI-formula exact for polynomials of a given total-degree, with cardinality increasing proportionally to the overall number of disks times the degree squared;
- allows then to compute immediately at machine precision some relevant features in applications, such as the area of the union and its first and second monomial moments (i.e. its “center of mass” and “moment of inertia” for a constant density);
- finally, provides a compressed PI-formula with cardinality not exceeding the dimension of the exactness polynomial space, irrespectively of the overall number of disks.

Acknowledgements

This work was partially supported by the DOR funds and the biennial project BIRD 192932 of the University of Padova, by the INdAM-GNCS 2022 Project “Methods and software for multivariate integral models”, and has been accomplished within the RITA Research Italian network on Approximation and the UMI Group TAA Approximation Theory and Applications.

References

- [1] D. Avis, B.K. Bhattacharya, H. Imai, Computing the volume of the union of spheres. *The Visual Computer*, 3:323–328, 1988.
- [2] B. Bauman, A. Sommariva, M. Vianello, Compressed cubature over polygons with applications to optical design. *J. Comput. Appl. Math.*, 370:112658, 2020.
- [3] B. Bauman, H. Xiao, Gaussian quadrature for optical design with noncircular pupils and fields, and broad wavelength range. *Proc. SPIE* 7652, 2010.
- [4] C. Caratheodory, Über den Variabilitätsbereich der Koeffizienten von Potenzreihen, die gegebene Werte nicht annehmen. *Math. Ann.*, 64:95–115, 1907.
- [5] G. Da Fies, A. Sommariva, M. Vianello, Algebraic cubature by linear blending of elliptical arcs. *Appl. Numer. Math.*, 74:49–61, 2013).
- [6] G. Da Fies, M. Vianello, Trigonometric Gaussian quadrature on subintervals of the period. *Electron. Trans. Numer. Anal.*, 39: 02–112, 2012.
- [7] G. Da Fies, M. Vianello, Algebraic cubature on planar lenses and bubbles. *Dolomites Res. Notes Approx. DRNA*. 5:7–12, 2012.
- [8] M. Dell’Orto, M. Dessole, F. Marcuzzi, The Lawson-Hanson Algorithm with Deviation Maximization: Finite Convergence and Sparse Recovery. *Numer. Linear Algebra Appl.*, accepted upon revision. arXiv:2108.05345v3, 2022.
- [9] M. Dessole, F. Marcuzzi, Deviation maximization for rank-revealing QR factorizations. *Numer. Algorithms*, 91:1047-1079, 2022.
- [10] M. Dessole, F. Marcuzzi, M. Vianello, Accelerating the Lawson-Hanson NNLS solver for large-scale Tchakaloff regression designs. *Dolomites Res. Notes Approx. DRNA*, 13:20–29, 2020.
- [11] S. Hayakawa, Monte Carlo cubature construction. *Jpn. J. Ind. Appl. Math.*, 38:561-577, 2021.
- [12] I.J. Kim, H. Na, An efficient algorithm calculating common solvent accessible volume. *PLoS ONE*, 17(3):e0265614, 2022.
- [13] C.L. Lawson, R.J. Hanson, Solving least squares problems. *Classics in Applied Mathematics* 15, SIAM, Philadelphia, 1995.
- [14] F. Librino, M. Levorato, M. Zorzi, An algorithmic solution for computing circle intersection areas and its applications to wireless communications. *Wireless Communications and Mobile Computing*, 14:1672–1690, 2014.

- [15] M. Petitjean, Spheres Unions and Intersections and Some of their Applications in Molecular Modeling. A. Mucherino & al., Eds., Distance Geometry: Theory, Methods, and Applications, Springer New York, pp.61-83, 2013.
- [16] F. Piazzon, A. Sommariva, M. Vianello, Caratheodory-Tchakaloff Subsampling. *Dolomites Res. Notes Approx. DRNA*, 10: 5–14, 2017.
- [17] D.L. Ragozin, Constructive Polynomial Approximation on Spheres and Projective Spaces. *Trans. Amer. Math. Soc.*, 162:157–170 (1971).
- [18] M. Slawski, Non-negative least squares: comparison of algorithms. <https://sites.google.com/site/slawskimartin/code>.
- [19] A. Sommariva, Software page with downloadable numerical codes. <http://www.math.unipd.it/~alvise/software.html>.
- [20] A. Sommariva, M. Vianello, Numerical quadrature on the intersection of planar disks. *FILOMAT*, 31(13):4105–4115, 2017.
- [21] A. Sommariva, M. Vianello, SUBP: Matlab package for subperiodic trigonometric quadrature and multivariate applications, online at: <https://www.math.unipd.it/~marcov/subp.html>.
- [22] A. Sommariva, M. Vianello, Compression of multivariate discrete measures and applications. *Numer. Funct. Anal. Optim.*, 36: 1198–1223, 2015.
- [23] A.H. Stroud, Approximate Calculation of Multiple Integrals. Prentice-Hall, 1971.
- [24] V. Tchakaloff, Formules de cubatures mécaniques à coefficients non négatifs, (French). *Bull. Sci. Math.*, 81:123–134, 1957.
- [25] M. Tchernychova, Caratheodory cubature measures. Ph.D. dissertation in Mathematics (supervisor: T. Lyons), University of Oxford, 2015.
- [26] X. Wu, S. Liu, W. Liu, T. Zhou, L. Wang, Comparison of three TCC calculation algorithms for partially coherent imaging simulation, Proc. SPIE 7544: 2010.